Conditioning of the Graphite Bumper Limiter for Enhanced Confinement Discharges in TFTR

H.F. Dylla, P.H. LaMarche, M. Ulrickson, R.J. Goldston,
D.B. Heifetz, K.W. Hill, and A. T. Ramsey
Princeton Plasma Physics Laboratory
P.O. Box 451,
Princeton, NJ 08544

PPPL--2448
DE87 013199

Abstract

A strong pumping effect has been observed with plasma operation on the toroidal graphite bumper limiter on TFTR. The pumping effect was induced by conditioning the limiter with a short series (10-20) of low density deuterium- or helium-initiated discharges. The density decay constant (τ_p^*) for gas-fueled ohmic discharges was reduced from $\tau_p^* > 10$ s before conditioning to a minimum value of $\tau_p^* = 0.15$ s after conditioning, corresponding to a reduction in the global recycling coefficient from ~ 100% to less than 50%. Coincident with the low recycling conditions, low current neutral-beam-fueled discharges show global energy confinement times which are enhanced by a factor of two over results with an unconditioned limiter. Two models are proposed for the observed pumping effects: (1) a depletion model based on pumping of hydrogenic species in the near-surface region of the limiter after depletion of the normally saturated surface layer by (carbon and helium) ion-induced desorption; and (2) a codeposition model based on pumping of hydrogenic species in carbon films sputtered from the limiter by the conditioning process.

1.0 Introduction

TFTR has been operating since September 1985 with a toroidal bumper limiter which covers a 120° poloidal segment of the inner wall. The bumper limiter is constructed of POCO® AXF-5Q graphite tiles, totals 2000 kg in mass, and presents a geometric surface area of approximately 22 m^2 to the torus vacuum [1]. The density of the graphite is about 1.8 g/cm^3, which is approximately 30% less than the maximum density of graphite. Recent laboratory measurements on the graphite tile material, including surface area measurements using rare gas adsorption [2] and hydrogen isotope retention measurements [3-7], indicate that the bulk porosity of the graphite is well connected to the surface. This property is expected to affect both the solubility and diffusivity of sorbed hydrogenic and impurity (primarily oxygen) species in the graphite, and hence affect the hydrogenic and impurity recycling properties of the limiter. We have developed new conditioning techniques for the bumper limiter for the purpose of reducing the impurity influx and for modifying the hydrogenic recycling properties.

For reducing impurities a new conditioning technique [8], dubbed "disruptive discharge cleaning" (DDC), has been developed which involves intentionally disrupting high power discharges against the bumper limiter. This procedure enhances water desorption by heating the bumper limiter to high surface temperatures (> 1000°C). The standard bakeout temperature of TFTR (150°C) and the surface heating due to heat deposition from typical ohmically heated discharges ($\lesssim$ 60°C) are insufficient to degas the large quantities of H_2O that are sorbed by the AXF-5Q graphite following atmospheric exposure [9].

For modifying the hydrogenic recycling properties we have found that the application of a short series (10-20) of low density, helium- or deuterium-initiated ohmic discharges reduces the recycling coefficient of the graphite

limiter leading to lower edge neutral densities. In subsequent neutral-beam-fueled discharges these modified edge conditions have resulted in a more peaked plasma density profile, and have led to energy confinement parameters which are enhanced by a factor of two over previously attained values [10-12].

2.0 Observed Change in Recycling

Recycling can be measured using the characteristic electron density decay constant, τ_p^*, defined by a plasma density decay factor of $\exp(-t/\tau_p^*)$ in the presence of no external sources, and a global electron recycling coefficient,

$$R = 1 - \tau_p/\tau_p^* \qquad (1)$$

which is a measure of the enhancement of τ_p^* over the globally-averaged core particle confinement time, τ_p. If τ_p^* is measured immediately after gas fueling is turned off, the calculated R may be assumed to be the same for both the electrons and the fueling gas.

Recycling conditions in TFTR illustrated in Fig. 1a were typical of all TFTR plasma operations on the moveable limiter, and were also characteristic of bumper limiter operations prior to the application of the low density conditioning discharges. In this ohmic discharge (Fig. 1a) the temporal response of the midplane line-averaged plasma density is compared to the gas-fueling rate. Gas input was usually required only during the density (and current) rise portion of the discharge. During the steady-state portion of the discharge, the gas input dropped to zero and the density was maintained at a slowly decaying level by recycling. The density decay constant, τ_p^*, measured after turning off the gas input, was greater than 10 s.

Figure 1b shows the change in recycling conditions observed after an initial conditioning of the bumper limiter with a series of ten, low density, 0.8 MA, He discharges. Gas input is required to maintain plasma densities above the minimal density, and when the gas input is intentionally terminated, the density decays with a time constant of $\tau_p^* = 2.0$ s. A global particle confinement time of $\tau_p = 0.1$ s was obtained from Dα emission and Langmuir probe measurements [13]. For the case shown in Fig. 1a, the value of R is greater than 99%. After the initial use of He conditioning, shown in Fig. 1b, the recycling coefficient falls to 96%. Figure 1c shows the case for the lowest recycling observed, i.e., after extensive conditioning of the bumper limiter using this low density discharge technique. The density decay constant was determined by the density decay to a baseline density following a 100 ms deuterium gas pulse during a 0.8 MA discharge (Fig. 1d). In this case the value of τ_p^* is 0.15 s, corresponding to a recycling coefficient of $R = 0.3 \pm 0.2$.

3.0 Comparison of Conditioning Sequences

Decreased recycling from the bumper limiter has been observed for several types of low density conditioning sequences, in addition to the short 0.8 MA He sequence described above. Having observed the effect with the initial use of He discharges, we undertook a more systematic investigation of the change in recycling conditions with extended exposure to low density discharges fueled by He or D_2 at varying plasma currents.

Figure 2 shows the shot-to-shot evolution of the minimum plasma density achieved in a series 0.8 MA D^+ conditioning discharges. The first sequence with D^+ discharges shows an initial rapid drop in plasma density after the first five discharges; but then during the remainder of this and two further

10-shot sequences, the density drop is less significant. Between the conditioning sequences, a short series of neutral-beam-injected (NBI) discharges were interspersed to test the effect of the conditioning on beam fueling.

Following the D^+ conditioning sequence, He^{++} conditioning sequences with plasma currents of 0.8 MA and 1.4 MA were applied as shown in Figs. 3a and 3b, respectively. In contrast to the D^+ sequences, the He^{++} sequences show a steady trend to lower plasma densities with increasing shot number. The lower densities achieved in the He^{++} discharges resulted in densities in subsequent 0.8 MA D^+ discharges which were below the apparent low density limit shown in Fig. 2. Figure 4 shows an expanded data base of the density vs. discharge number which spans a 1000-shot interval covering the initial 0.8 MA D^+ conditioning sequence (Fig. 2) followed by the 0.8 MA, 1.4 MA (Fig. 3) and 1.8 MA (not shown) He^{++} conditioning sequences. The density fell from 0.87×10^{19} m^{-3} to 0.54×10^{19} m^{-3} during this interval, and there is some indication that the minimum attainable density decreases with the current of the He^{++} conditioning discharges. According to spectroscopic analysis of these low density discharges (both He and D_2 initiated), the dominant impurity is carbon and the measured values of Z_{eff} are equal to 6 within the estimated error (± 15%) of the measurements [14,15]. Metals are estimated to contribute a value of 0.6 ± 0.3 to Z_{eff}; thus a Z_{eff} of 6 does not imply a pure carbon discharge or a total absence of deuterium.

The effectiveness of the conditioning discharges for degassing the limiter of deuterium is shown in Fig. 5, where the Dα emission line brightness, which is proportional to the D influx, decreases by a factor of 20 during this sequence. The cause of the two different decay constants (τ) observed in the decrement of Dα emission with shot number is unknown.

Variations in the decay constant have been observed during other conditioning sequences, possibly indicating that the time dependence of the deuterium degassing process depends on the initial deuterium retention conditions of the limiter.

The effect of the conditioning sequences on the recycling behavior of gas- and neutral-beam-fueled discharges is shown in Figs. 6, 8-10. Figure 6 shows the evolution of the density decay constant (τ_p^*) over a span of 100 discharges, which includes the conditioning sequence shown in Figs. 2 and 3. These measurements were obtained during fiducial discharges which were interspersed within the conditioning sequence. The fiducial discharges were programmed to a density of $\bar{n}_e = 1.25 \times 10^{19}$ m^{-3}, followed by a programmed interruption of the deuterium gas input at 2.0 s to allow the density to decay to the recycling limit. We assume here that the measured plasma density decay constant, τ_p^*, is representative of the decay in deuteron density, since the τ_p^* measurement follows the termination of deuterium gas injection. Over this discharge sequence the data in Fig. 6 show that τ_p^* decreased from an initial value of 1.2 s to a minimum value of 0.29 s.

The corresponding change in the global recycling coefficient, R, was determined by solving

$$\frac{dN}{dt} = \dot{N}_R - \frac{N}{\tau_p} \qquad (2)$$

for τ_p and Eq. (1) for R. The total deuterium ion population, N, inside the last closed flux surface at r = 0.8 m was determined from measurements of $\bar{n}_e$ (assuming a parabolic profile) and Z_{eff}. The rate $\dot{N}_R$ at which recycling neutrals reionized within r = 0.8 m was estimated from Dα emission measurements from four detectors viewing the inner limiter. A two-dimensional

simulation was made of the neutral particle transport using the DEGAS code [16] to correct the Dα signals to include only contributions from neutral atoms and molecules ionized within r = 0.8 m. (Toroidal variations in the Dα signal were measured to be of the order of ± 10% and, therefore, were ignored.) The corrected Dα signals were then multiplied by ratios of ionizations per Dα photon calculated from the same simulation to compute $\dot{N}_R$.

Using the computed value of τ_p = 0.14 ± 0.04 s for this plasma current and density (Fig. 7), we calculated that the drop in τ_p^* over the conditioning sequence shown in Figs. 2 and 3 indicates a drop in global recycling from R ≈ 0.9 to R = 0.50 ± 0.15.

Further evidence of reduced recycling as a result of the bumper limiter conditioning comes from edge neutral pressure and edge neutral flux (from Dα emission) measurements. Figure 8 shows the observed drop in edge neutral pressure [17] and Dα emission for the conditioning sequence shown in Figs. 2 and 3. The measurements were made at the torus outer midplane during the plasma density plateau (t = 2.0 s) of fiducial discharges. A significant drop (a factor of ~ 15 for the edge pressure and a factor of ~ 25 for Dα) is evident as a result of the limiter conditioning.

The effect of reduced recycling is illustrated by the time variation of the edge neutral pressure, plasma density, and required gas input for gas-fueled (fiducial) discharges in Fig. 9 and neutral-beam-fueled discharges in Fig. 10. The data in Figs. 9 and 10 are taken from discharges occurring during the beginning and end of the conditioning sequence shown in Figs. 2 and 3 to illustrate the changes from high recycling (R ≈ 1) to low recycling conditions (R ≈ 0.5).

The observed decrease in recycling after limiter conditioning is not a permanent effect. The recycling coefficient can be increased by exposure of

the limiter to high density discharges. This gas-loading effect has been quantified by exposing a conditioned limiter to a series of nominally identical ohmic discharges at the fiducial density ($\bar{n}_e$ = 1.25 x 10^{19} m^{-3}). Starting from conditions where R = 0.5, exposure to ten fiducial discharges increased the recycling coefficient to R = 0.8. Over this same discharge sequence the gas input required to fuel the discharge decreased from 40 torr-liters to an asymptotic value of 20 torr-liters per discharge. By summing the gas input required for the entire sequence and subtracting the minimum (asymptotic) gas fueling of 20 torr-liters per discharge, we obtained a measurement of ≈ 100 torr-liters for the pumping capacity of the conditioned bumper limiter for ohmic plasma.

4.0 Discussion

It is evident from the density decay time constant, edge neutral pressure, and Dα emission measurements that exposure of the bumper limiter to an extended series of low density discharges significantly reduces the recycling. The low density limit for these conditioning discharges, which are fueled with the minimal amount of gas to satisfy discharge breakdown, was reduced by approximately a factor of two. Subsequent conditioning sequences, which followed exposure of the limiter to high density gas- and pellet-fueled discharges, showed reductions by factors of three in the density limit.

A detailed explanation of the relationship between reduced recycling and the low density discharge conditioning process is a subject of current study. Two models are discussed here which account for the observed drop in recycling as the result of a pumping capability induced in the graphite limiter material by the conditioning discharges: (1) a depletion model based on deuterium adsorption-desorption in the near surface region of the bumper

limiter, and (2) a codeposition model based on deuterium adsorption in carbon films formed by material sputtered from the limiter.

The hydrogenic retention property of graphites, such as the TFTR limiter material, is the subject of recent investigation [3-7,18-19]. For AXF-5Q (and similar) graphites at room temperature the saturation concentration, D/C, is approximately 0.4, and this limiting concentration falls rapidly with increasing temperature [18, 19]. Below the saturation concentration, incident deuterium that penetrates the lattice is retained (i.e., pumped) at low graphite temperatures. The saturation volume and, hence, the pumping capacity depend on the implantation depth of the incident deuterium. For typical edge electron temperatures ($T_e(a) \approx 75$ eV estimated for TFTR low density discharges [20], the impacting ion energy of deuterium incident onto the limiter is of the order of ~ 200 eV, and the implantation depth of such particles is ~ 10 nm [21].

The first model of graphite limiter pumping explains the pumping effect simply as the result of deuterium retention by a nonsaturated near-surface region of the limiter. The active volume is the product of the scrape-off area of the limiter and the implantation depth. In the unconditioned state this implantation volume of the bumper limiter is saturated; therefore, the pumping capacity is zero and the limiter recycling coefficient is close to unity.

The conditioning process with the low density discharges partially depletes the hydrogen within the implantation volume by an ion impact desorption process. The incident particle which initiates the desorption process can be a hydrogenic ion, helium ion, or carbon ion since spectroscopic analysis and the measured Z_{eff} (5-6) of the conditioning discharges indicate that both the helium- and deuterium-initiated discharges have significant carbon ion content.

The replacement of an implanted hydrogenic species in carbon by a different isotope is well documented in the literature [22]. The hydrogen isotope exchange process can be optimized by matching the implantation range of the incident particle with the depth of the implanted isotope by adjustment of the incident particle velocity. Such one-for-one interchange of hydrogen isotopes cannot result in a net depletion of the saturated layer; however, the helium flux in the helium-fueled discharges and the carbon flux in both types of conditioning discharges (helium or deuterium initiated) are expected to cause a net depletion of hydrogenic species [23].

Recently, Wampler, Doyle, and Brice [24] have measured the rate of deuterium depletion in carbon by helium and carbon ion-induced desorption. Using graphite samples that have been implanted to saturation by exposure to a 10^{17} cm^{-2} fluence of 300 eV deuterium ions, Wampler et al. [24] measured a depletion of ~ 12% of the implanted deuterium after a fluence of 10^{16} cm^{-2}, 600 eV He ions, and a depletion of ≈ 33% of the implanted deuterium after a fluence of 10^{16} cm^2, 3 keV C^+ ions (Fig. 11). These data indicate that carbon ions are more efficient in releasing deuterium from the saturated surface of graphite, and thus ion-induced desorption by carbon ions probably plays the dominant role in the limiter conditioning process.

This depletion model of graphite pumping accounts for the observed transient nature of the reduction in recycling and our inability to observe strong pumping effects with plasma operation on the TFTR moveable limiter. The pumping capacity of the depleted layer on the bumper limiter is limited, and is estimated to be the same as the gas loading (~ 100 torr liters) of ten fiducial density discharges, which was demonstrated to saturate the pumping effect.

Limiter pumping, as manifest by less than unity recycling, has not been observed with plasma operation on the TFTR moveable limiter. We have not observed values of the density decay constant, τ_p^* less than 8 s after conditioning the moveable limiter with low density discharges. There are several reasons to expect the recycling on the moveable limiter to be near unity during much of the steady-state portion of a high power discharge. The smaller limiter scrape-off area (~ 0.4 m^2), which is an order of magnitude smaller than the bumper limiter scrape-off area (~ 5 m^2), results in a smaller saturation capacity. The higher bulk limiter temperature (< 800°C for ohmic discharges on the moveable limiter, compared to <60°C for the bumper limiter) results in a further reduction of the saturation capacity. Using the 3-D neutral transport code, DEGAS [16], Heifetz et al. [25,26] have calculated that the recycling coefficient on the moveable limiter reaches unity in less than 0.5 s after the initiation of a typical TFTR ohmically heated discharge.

As seen with the bumper limiter conditioning, we have observed that exposure of the moveable limiter to a low density conditioning discharge sequence does remove gas from the limiter and lower the minimum achievable plasma density. In fact, this conditioning procedure was first attempted in TFTR with the moveable limiter and led to the discovery of the enhanced confinement mode [10]. The apparent differences in limiter recycling effects observed with operation on the moveable or bumper limiter, and the relationship between limiter conditioning and the enhanced confinement discharges are active topics for further investigation.

A second model for graphite limiter pumping attributes the pumping effect to adsorption in a carbon film sputtered onto the vessel surfaces by the conditioning discharges (Wilson and Hsu [7] and Winter [27]). In-situ observations and measurements in tokamaks with graphite limiters [2,8,27-29],

and laboratory measurements with hydrogenic glow discharges with graphite electrodes [5,6] show that significant quantities of carbon can be sputtered from the bulk graphite and redeposited as a carbonaceous film on vessel surfaces. Sputtered carbon can also be redeposited onto lower particle flux regions of the limiter. The sputtering processes in the conditioning discharges by the carbon and helium ions are more efficient than sputtering by deuterium ions. At an impacting ion energy of 300 eV the physical sputtering coefficients for C^+, He^+, and D^+ are 0.23, 0.077, and 0.024, respectively, [30,31] and the actual physically sputtered flux in TFTR should show a larger variation at a given sheath potential because of the probable multiply charged states of He (He^{++}) and C (CIV-CV). At higher limiter temperatures (such as with the case of moveable limiter operation in TFTR) erosion yields by hydrogenic species can be enhanced by chemical sputtering or radiation-enhanced sublimation [32].

To test the plausibility of this codeposition model for the pumping effects observed in TFTR, we estimated the capacity of the redeposited films to pump hydrogenic species using data from wall samples that were removed from the TFTR vessel in March 1986. These wall samples were distributed poloidally and toroidally and were exposed to the initial vacuum vessel conditioning at the beginning of the run [8], followed by ~ 1770 high power, deuterium-fueled discharges. Net deposition of a carbonaceous film was measured on all the samples, with a composition: 80-90 at.% C, 6-10 at.% O, 1-6 at.% D, and 1 at.% metals. The average carbon deposition was 3.5×10^{18} cm^{-2}, and the average D deposition was 1.3×10^{17} cm^{-2}, yielding an approximate 4% saturation of the film. If we multiply the average sample loading of D per discharge (7.3×10^{13} cm^{-2}) by the vessel wall area (~ 200 m^2), the observed wall loading corresponds to a wall pumping of D per discharge of 1.5×10^{20}

(≈ 5 torr-liters). Considering the crudity of these numerical estimates and the fact that the deposited film is capable of roughly a factor of ten larger hydrogenic loading, we cannot discount the codeposition model as a contributing source of wall and/or limiter pumping in TFTR. However, preliminary results from a 3-D particle transport calculation of a bumper limiter discharge [26] indicate that only 1-5% of the total hydrogenic flux impacts wall areas beyond the bumper limiter. Therefore, even though the deposited films on the vessel wall may have the capacity for pumping, our initial estimate of the incident hydrogenic flux is too low to account for the observed pumping effects.

5.0 Conclusions

We have described the pumping effects observed with operation of the toroidal graphite bumper limiter in TFTR. The pumping effects are induced by conditioning the limiter with a series of low density helium- or deuterium-initiated discharges. The following pumping effects are observed to occur with conditioning of the bumper limiter: (1) During gas-fueled ohmic discharges, the effective particle confinement time, τ_p^*, decreases from $\tau_p^* >$ 10 s to a minimum value of $\tau_p^* = 0.15$ s; this decrease in τ_p^* corresponds to a decrease in global recycling from $R \approx 1$ to $R \leq 0.5$; (2) the minimum plasma density sustained at low plasma currents (~ 1 MA) decreases by a factor of two; (3) the edge neutral pressure and recycling flux during neutral beam fueling decreases by almost an order of magnitude. Subsequent neutral beam heating experiments into low density target plasmas with a conditioned (i.e., low recycling) limiter have shown energy confinement times which are enhanced by a factor of two over previous values obtained with an unconditioned (i.e., high recycling) limiter [10-12].

We have proposed two mechanisms for the observed pumping effects: (1) a depletion model based on pumping of the hydrogenic species in the near-surface region of the bumper limiter, and (2) a codeposition model based on pumping by carbon films sputtered from the limiter by the conditioning. Considering that the pumping effects have been observed only with plasma operation on the large area bumper limiter (which operates near 60°C) and that the pumping capacity (≈ 100 torr-liters) is consistent with the hydrogenic capacity of the depletion layer, we favor the depletion model as the primary cause of the pumping effects observed in TFTR.

Acknowledgements

We acknowledge D.K. Owens and M. Bell for their help in developing the concept for helium conditioning discharges. The use of low density deuterium conditioning discharges was first explored on the moveable limiter by J. Strachan. The authors wish to thank our colleagues at Sandia National Laboratory, D. Brice, B.L. Doyle, W.L. Hsu, A. Pontau, W. Wampler, and K. Wilson for their contributions to this study, and for providing the data of Ref. 24 prior to publication. The authors thank R. Hawryluk, D. Manos, F. Wagner, and M. Zarnstorff for useful discussions and participation in the experimental studies. This work was supported by US DOE Contract No. DE-AC02-76-CH03073.

References

[1] L. Sevier, M.F. Ho, J. Citrolo, J. Bialek, D. Wiessenburger, and I. Zatz, Proc. 10th Symp. on Fusion Energy, Philadelphia 1983 (IEEE, NY 1984) pp. 1072-1076.

[2] A.E. Pontau, W.R. Wampler, B.E. Mills, B.L. Doyle, A.F. Wright et al., J. Vac. Sci. Technol. A4 (1986) 1193.

[3] R.A. Causey, M.I. Baskes, and K.L. Wilson, J. Vac. Sci. Technol. A4 (1986) 1189.

[4] R.S. Strehlow, J. Vac. Sci. Technol. A4 (1986) 1183.

[5] W.L. Hsu and R.A. Causey, Proc. 10th Intern. Vacuum Congress and 33rd National Symp. of the American Vacuum Society, Baltimore, October 1986, J. Vac. Sci. Technol. A. (in press).

[6] R.A. Langley, op. cit.

[7] K.L. Wilson and W.L. Hsu, J. Nucl. Mater. 145/147 (1987) 121.

[8] H.F. Dylla and the TFTR Team, J. Nucl. Mater. 145/147 (1987) 48.

[9] A.E. Pontau and D.H. Morse, J. Nucl. Mater. 141/143 (1986) 124.

[10] J.D. Strachan, M. Bitter, A.T. Ramsey, M.C. Zarnstorff, V. Arunasalam et al., Phys. Rev. Lett. 58 No. 10 (1987) 1004.

[11] R.J. Hawryluk, V. Arunasalam, M.G. Bell, M. Bitter, W.R. Blanchard et al., Proc. 11th Intern. Conf. on Plasma Physics and Contr. Nucl. Fusion Research, Kyoto, November 1986 (IAEA, Vienna) paper no. IAEA-CN-47/A-I-3.

[12] R.J. Goldston, op. cit., paper no. IAEA-CN-47/A-II-1.

[13] M. Shimada, A.T. Ramsey, D.K. Owens, H.F. Dylla, R.V. Budny, et al., J. Nucl. Mater. 145/147 (1987) 544.

[14] A.T. Ramsey and S.L. Turner, Rev. Sci. Instrum. (in press)

[15] K.W. Hill, V. Arunasalam, M.G. Bell, M. Bitter, W.R. Blanchard et al., Proc. 11th Intern. Conf. on Plasma Phys. and Contr. Nucl. Fusion Research, Kyoto, November 1986 (IAEA, Vienna) paper no. IAEA-CN-47/A-IV-2.

[16] D.B. Heifetz, J. Comput. Phys. 46 (1982) 309.

[17] P.H. LaMarche, H.F. Dylla, D.K. Owens, N.D. Arnold, W.J. Hojsak et al., Rev. Sci. Instrum. 56 (1985) 981.

[18] B.L. Doyle, W.R. Wampler, and D.K. Brice, J. Nucl. Mater. 103/104 (1981) 513.

[19] M. Braun and B. Emmoth, J. Nucl. Mater. 128/129 (1984) 657.

[20] R.V. Budny, D.B. Heifetz, S. Kilpatrick, D. Manos, D.K. Owens et al., J. Nucl. Mater. 145/147 (1987) 245.

[21] Calculated from TRIM 86 computer code (D.K. Brice, Sandia National Laboratories, 1986).

[22] D.K. Brice, B.L. Doyle, and W.R. Wampler, J. Nucl. Mater. 111/112 (1982) 598.

[23] W.R. Wampler and S.M. Myers, J. Nucl. Mater. 111/112 (1982) 616.

[24] W.R. Wampler, B.L. Doyle, and D.K. Brice, (private communication).

[25] D.B. Heifetz, H.F. Dylla, M. Ulrickson and M.I. Baskes, J. Nucl. Mater. 145/147 (1987) 326.

[26] D.B. Heifetz, H.F. Dylla, M. Ulrickson, and M.I. Baskes, Bull. Am. Phys. Soc. 31 (1986) 1448.

[27] J. Winter, Proc. 10th Intern. Vac. Congress and 33rd National Symp. Am. Vac. Soc., J. Vac. Sci. Technol. (in press).

[28] J.P. Coad, B.J. Davies, G.J. Edge, G.M. McCracken, and J. von Seggern, J. Nucl. Mater. 145/147 (1987) 747.

[29] H.F. Dylla, M.A. Ulrickson, P.H.LaMarche, D.K. Owens, and B.L. Doyle, J. Vac. Sci. Technol. A3 (1985) 1105.

[30] E. Hechtl, J. Bohdansky, and J. Roth, J. Nucl. Mater 103/104 (1981) 333.

[31] J. Roth, J. Bohdansky and W. Ottenberger, "Data on Low Energy Light Ion Sputtering," Report IPP 9/26 (May, 1979) Max-Planck-Institut für Plasmaphysik, Garching.

[32] J. Roth in Physics of Plasma-Wall Interactions in Controlled Fusion, D.E. Post and R. Behrisch, eds. (Plenum, New York, 1986) pp. 389-412.

[33] B.L. Doyle, W.R. Wampler, D.K. Brice, and S.T. Picraux, J. Nucl. Mater. 93/94 (1980) 551.

[34] P.C. Efthimion, N.L. Bretz, M.G. Bell, M. Bitter, W.R. Blanchard, Proc. 10th Intern. Conf. on Plasma Phys. and Contr. Nucl. Fusion Research London, UK September 1984 (IAEA, London) (IAEA, Vienna, Austria, 1985), Vol. 1, pp. 29-54.

Figure Captions

Fig. 1 Plasma density and gas input behavior for three operational cases in TFTR (a) standard conditions on moveable limiter or bumper limiter when recycling is close to one and the density decay constant (τ_p^*) is > 10 s. (b) 1.4 MA discharge on the bumper limiter (R/a = 2.45 m/0.80 m) after the initial conditionirg with ten low density He discharges. (c) 0.8 MA discharge on bumper limiter after extensive conditioning showing the lowest observed value of τ_p^* = 0.15 s (d).

Fig. 2 Change in the line-averaged plasma density of 0.8 MA deuterium-fueled conditioning discharges. The discharges were fueled only with a small (~ 3 torr-liter) gas fill prior to discharge initiation. During the breaks in the shot number sequence (x-axis), neutral-beam-fueled discharges were made to test the level of conditioning.

Fig. 3 Change in the line-averaged plasma density of 0.8 MA (a) and 1.4 MA (b) helium-fueled conditioning discharges. The discharges were fueled with a 2 torr-liter prefill of the torus.

Fig. 4 Change in the line-averaged plasma density of 0.8 MA deuterium-fueled discharges (prefill fueling only) over a 1000-shot sequence which spans conditioning sequences shown in Figs. 2 and 3.

Fig. 5 Reduction in brightness of the D_β emission and line-averaged plasma density during a sequence of 1.4 MA He conditioning discharges.

Fig. 6 Change in the density decay constant (τ_p^*) and computed value of the global recycling coefficient (R) over a 100-shot sequence which spans the conditioning sequence shown in Figs. 2 and 3. These measurements were made using fiducial discharges that were interspersed within the conditioning sequence. The plasma density was programmed to $\bar{n}_e$ = 1.25 x 10^{19} m^{-3} prior to interruption of the deuterium gas input to allow the density to decay.

Fig. 7 Particle confinement time (τ_p) as a function of line-averaged plasma density for 0.8 MA ohmic discharges on the bumper limiter. The values of τ_p were derived from absolute Dα emission measurements (see text). For comparison, values of the global energy confinement time, $\tau_E(a)$, calculated according to the description in Ref. 34 are also plotted.

Fig. 8 Change in the edge neutral pressure and Dα emission over the conditioning sequence shown in Figs. 2 and 3. These measurements were made at the torus outer midplane during the plasma density plateau of the fiducial discharges described in Fig. 6. The error bars in the pressure data are indicative of the noise level of the measurements.

Fig. 9 Time dependence of the edge neutral pressure, plasma density, and required gas input for fiducial discharges at the beginning (a,b) and end (c,d) of the conditioning sequence shown in Figs. 2 and 3.

Fig. 10 Time dependence of the edge neutral pressure, plasma density, and required gas input for neutral-beam-fueled discharges at the beginning (a,b) and end (c,d) of the conditioning sequence shown in Figs. 2 and 3.

Fig. 11 Ion-induced release of deuterium from graphite by 600 eV He and 3.0 keV C ions. The sample was saturated with 300 eV D prior to the release measurements. The 300 eV H data points were calculated using the local mixing model [33]. These data provided courtesy of Wampler, Doyle, and Brice [24], Sandia National Laboratory.

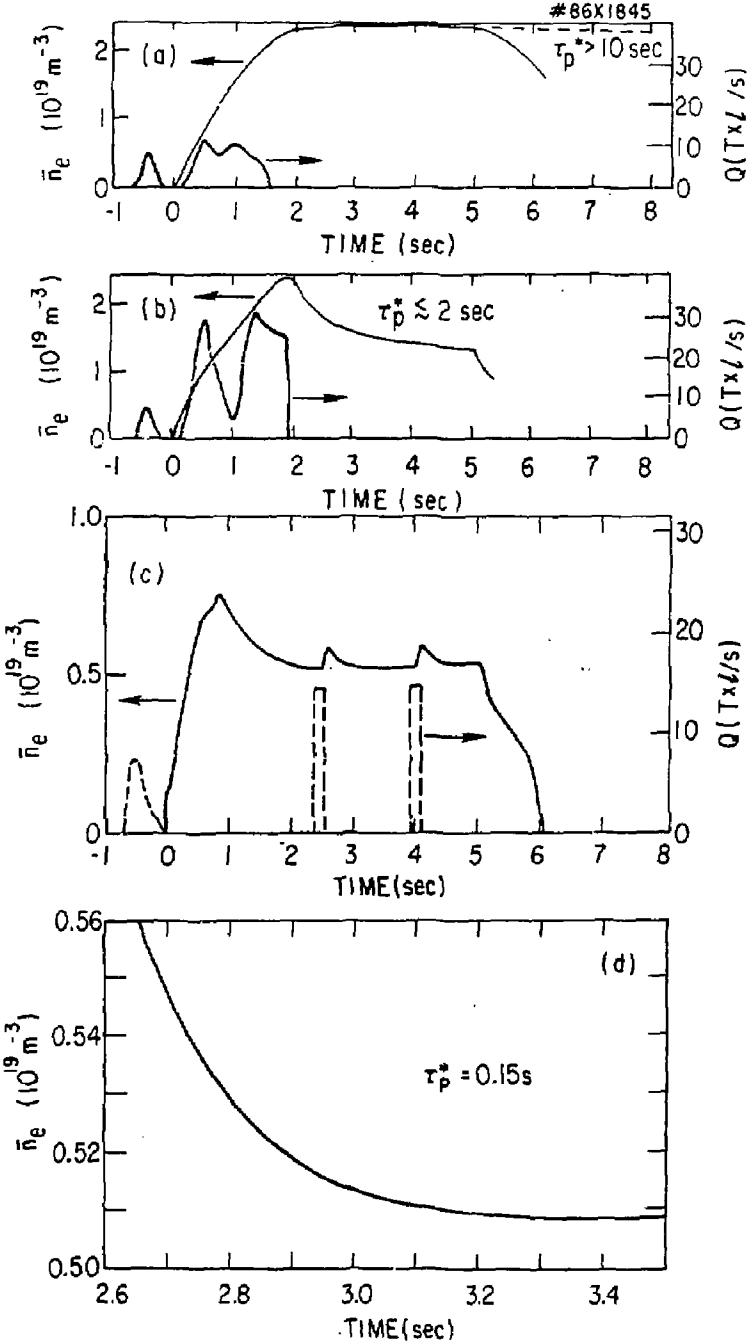
#86X1845
(a)
$\tau_p^* > 10$ sec
$\bar{n}_e$ (10^{19} m^{-3})
Q(Txℓ/s)
TIME (sec)
(b)
$\tau_p^* \lesssim 2$ sec
(c)
(d)
$\tau_p^* = 0.15$s

Fig. 1

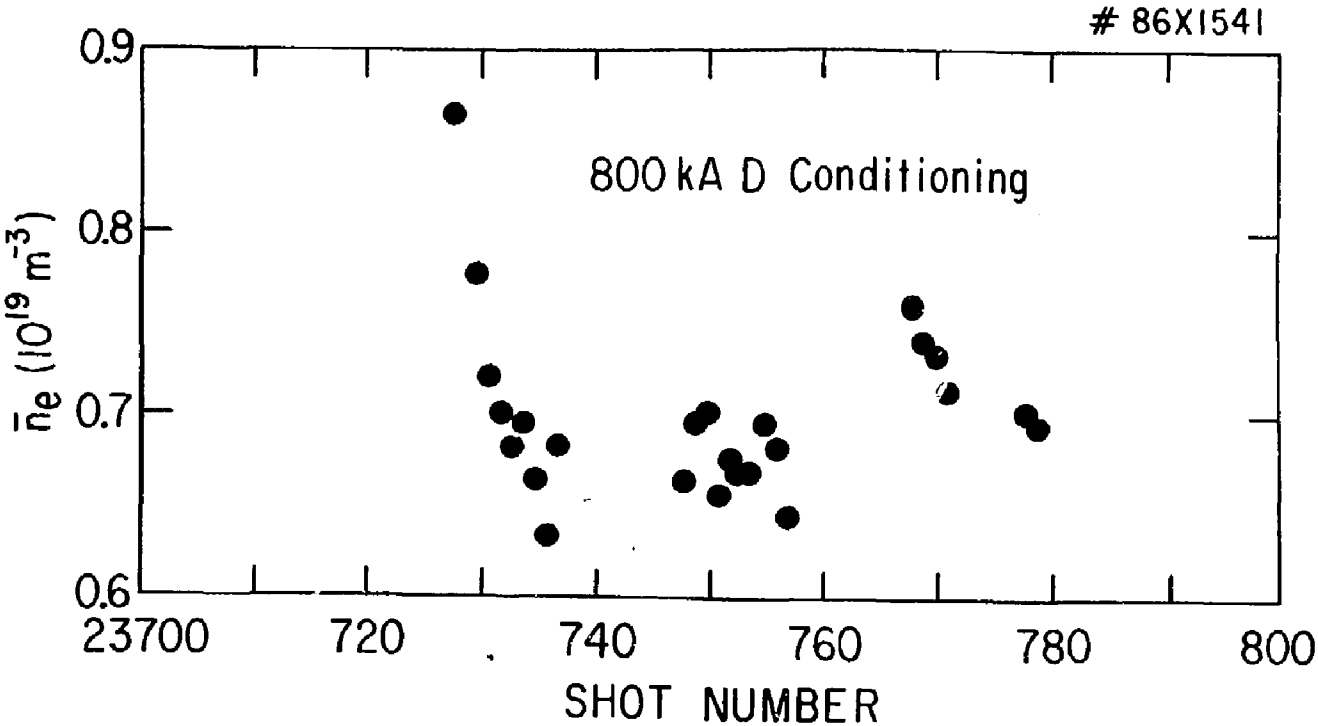
86X1541
800 kA D Conditioning
$\bar{n}_e$ (10^{19} m^{-3})
0.9
0.8
0.7
0.6
23700
720
740
760
780
800
SHOT NUMBER

Fig. 2

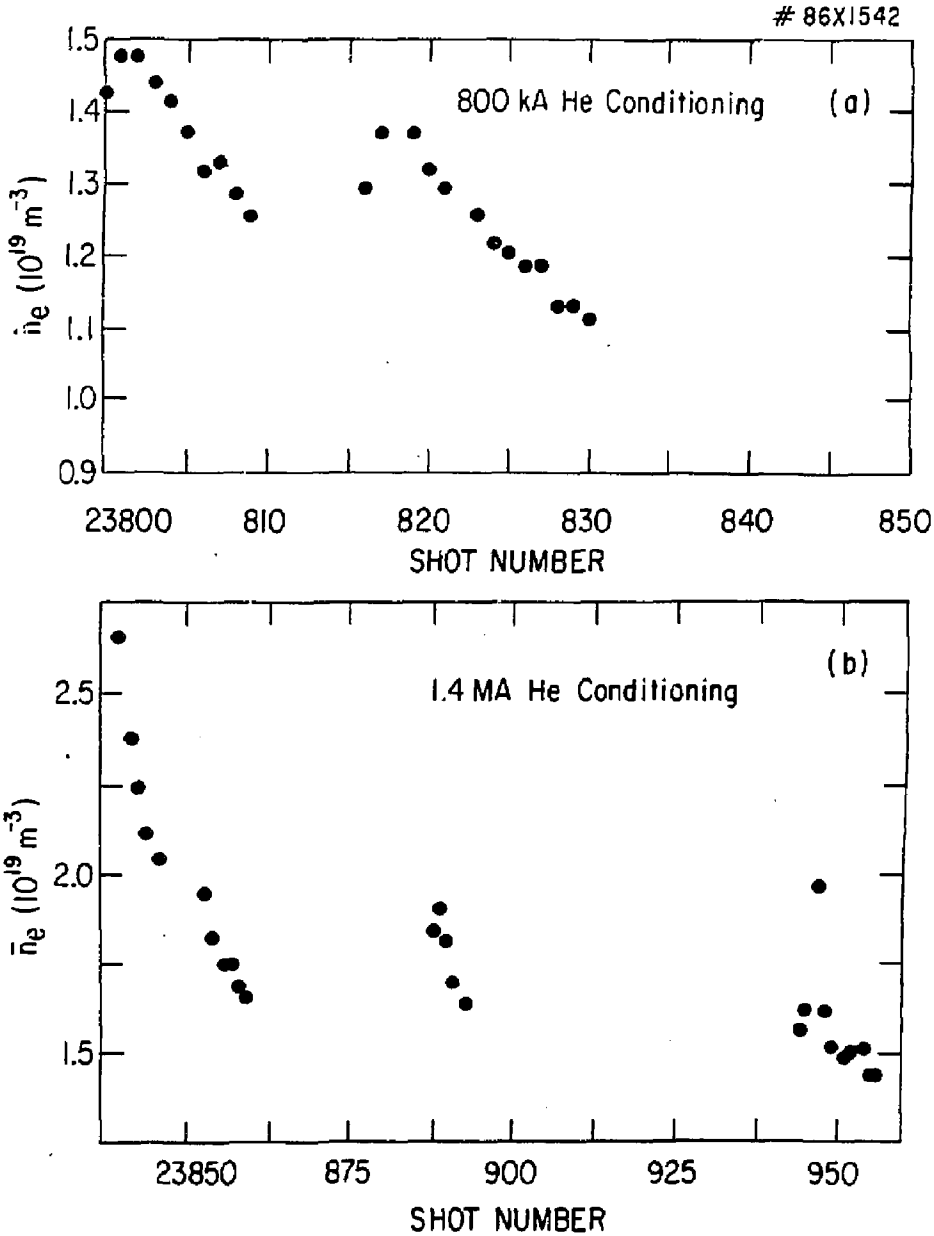
86X1542
800 kA He Conditioning
(a)
$\bar{n}_e$ (10^{19} m^{-3})
1.5
1.4
1.3
1.2
1.1
1.0
0.9
23800
810
820
830
840
850
SHOT NUMBER
(b)
1.4 MA He Conditioning
$\bar{n}_e$ (10^{19} m^{-3})
2.5
2.0
1.5
23850
875
900
925
950
SHOT NUMBER

Fig. 3

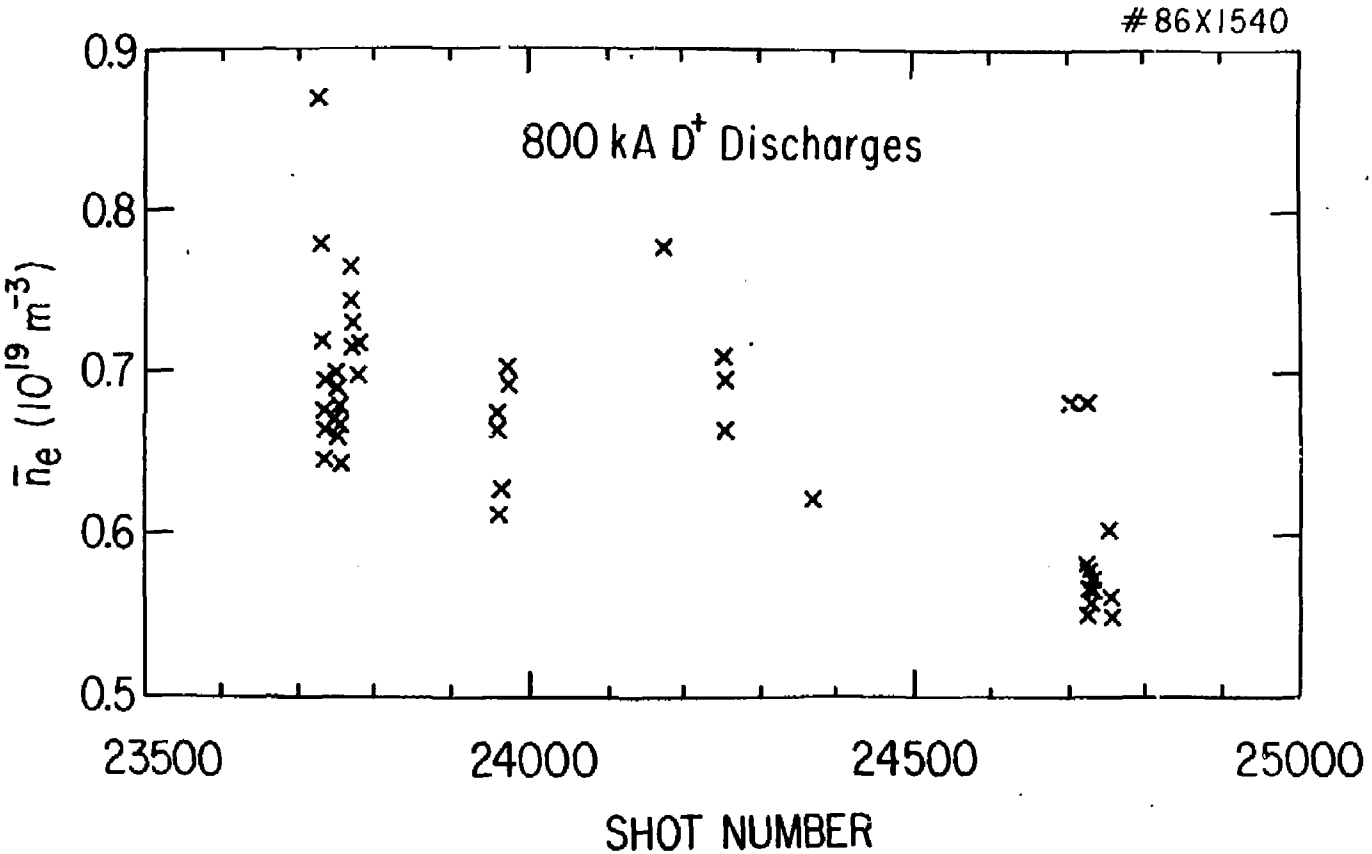
#86X1540
800 kA D+ Discharges
0.9
0.8
0.7
0.6
0.5
$\bar{n}_e$ (10^{19} m^{-3})
23500
24000
24500
25000
SHOT NUMBER

Fig. 4

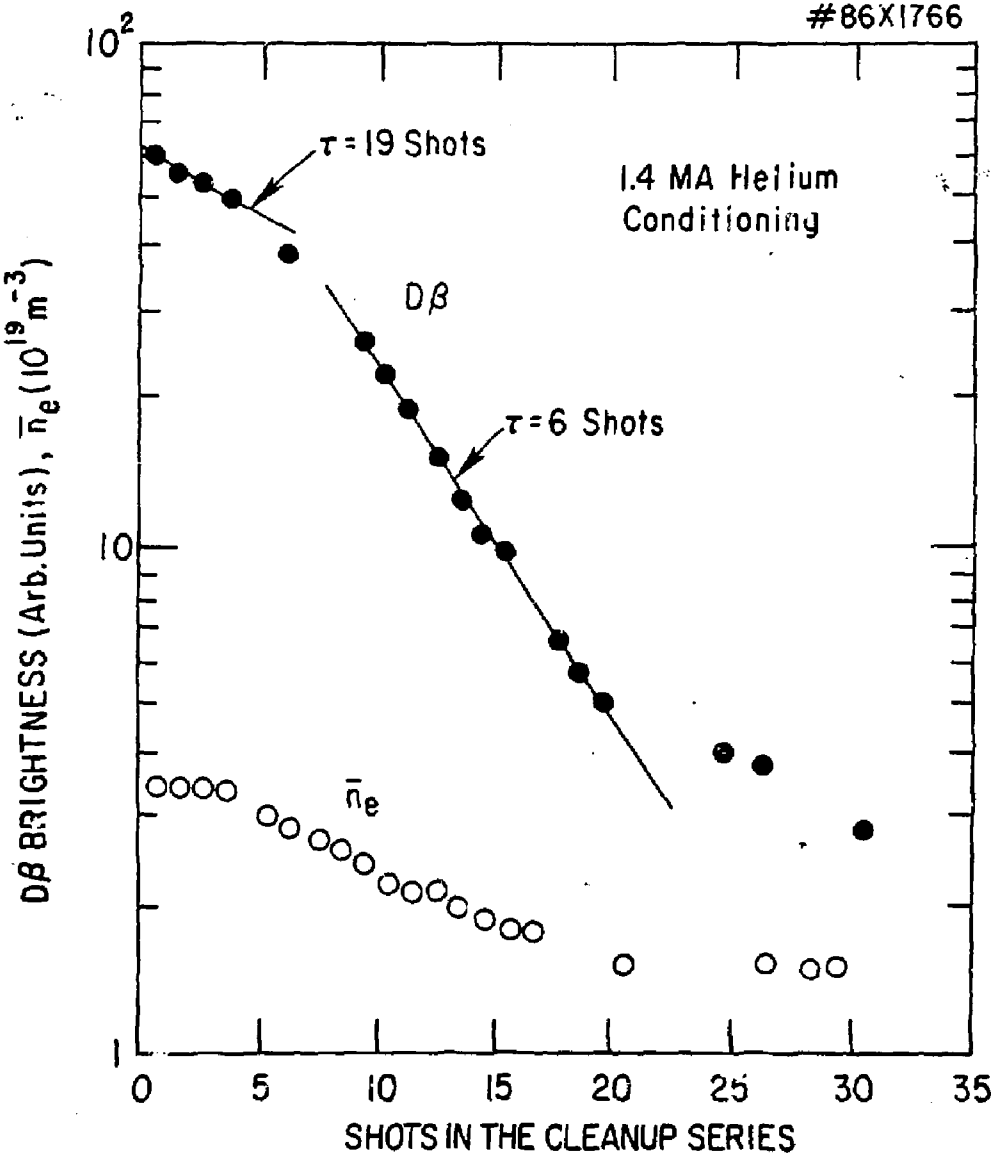
#86X1766
10^2
10
1
τ = 19 Shots
1.4 MA Helium
Conditioning
Dβ
τ = 6 Shots
$\bar{n}_e$
0
5
10
15
20
25
30
35
SHOTS IN THE CLEANUP SERIES
Dβ BRIGHTNESS (Arb.Units), $\bar{n}_e$ (10^{19} m^{-3})

Fig. 5

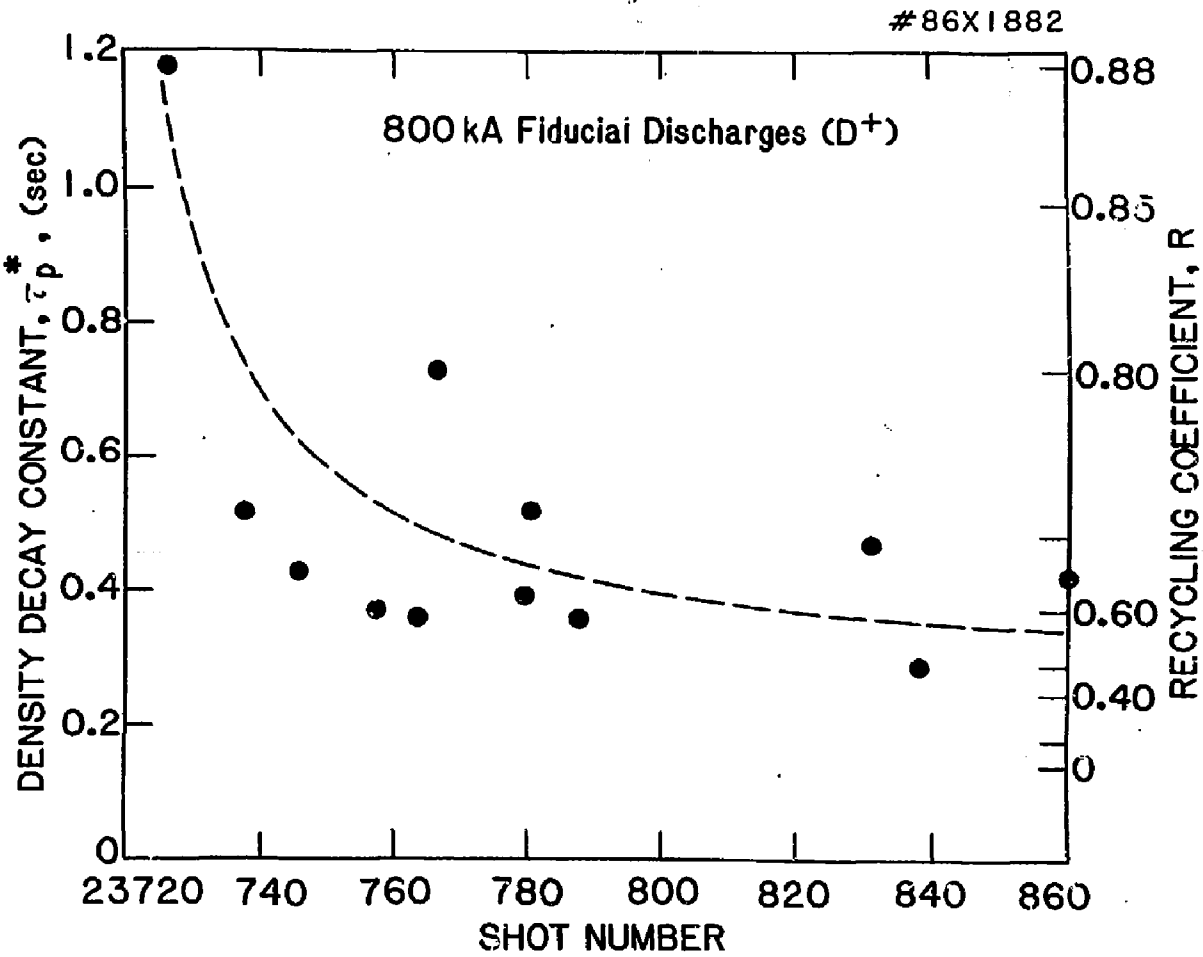
#86X1882
800 kA Fiduciai Discharges (D+)
DENSITY DECAY CONSTANT, τ*p, (sec)
RECYCLING COEFFICIENT, R
SHOT NUMBER
1.2
1.0
0.8
0.6
0.4
0.2
0
0.88
0.85
0.80
0.60
0.40
0
23720
740
760
780
800
820
840
860

Fig. 6

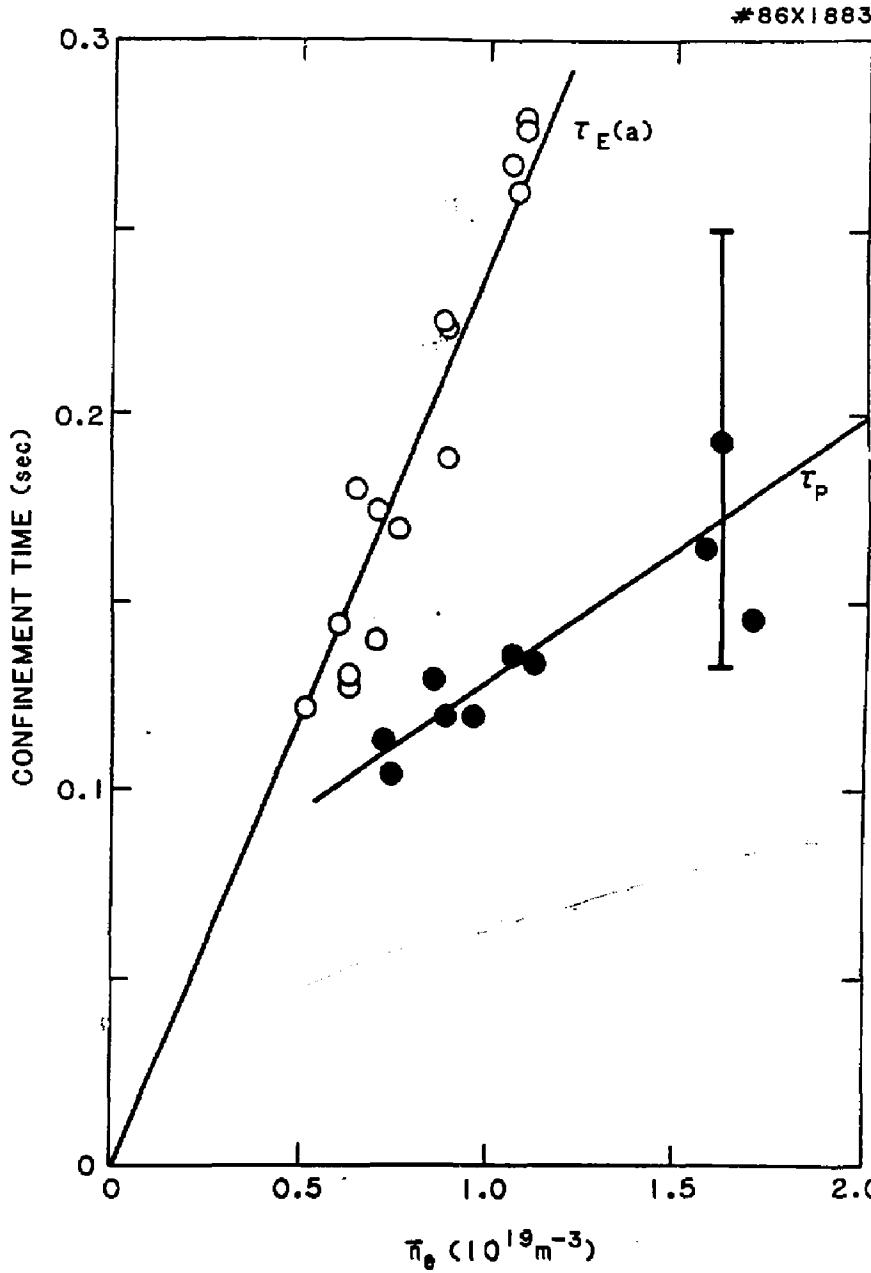
#86X1883
0.3
0.2
0.1
0
CONFINEMENT TIME (sec)
$\tau_E(a)$
τ_p
0
0.5
1.0
1.5
2.0
$\bar{n}_e$ ($10^{19}m^{-3}$)

Fig. 7

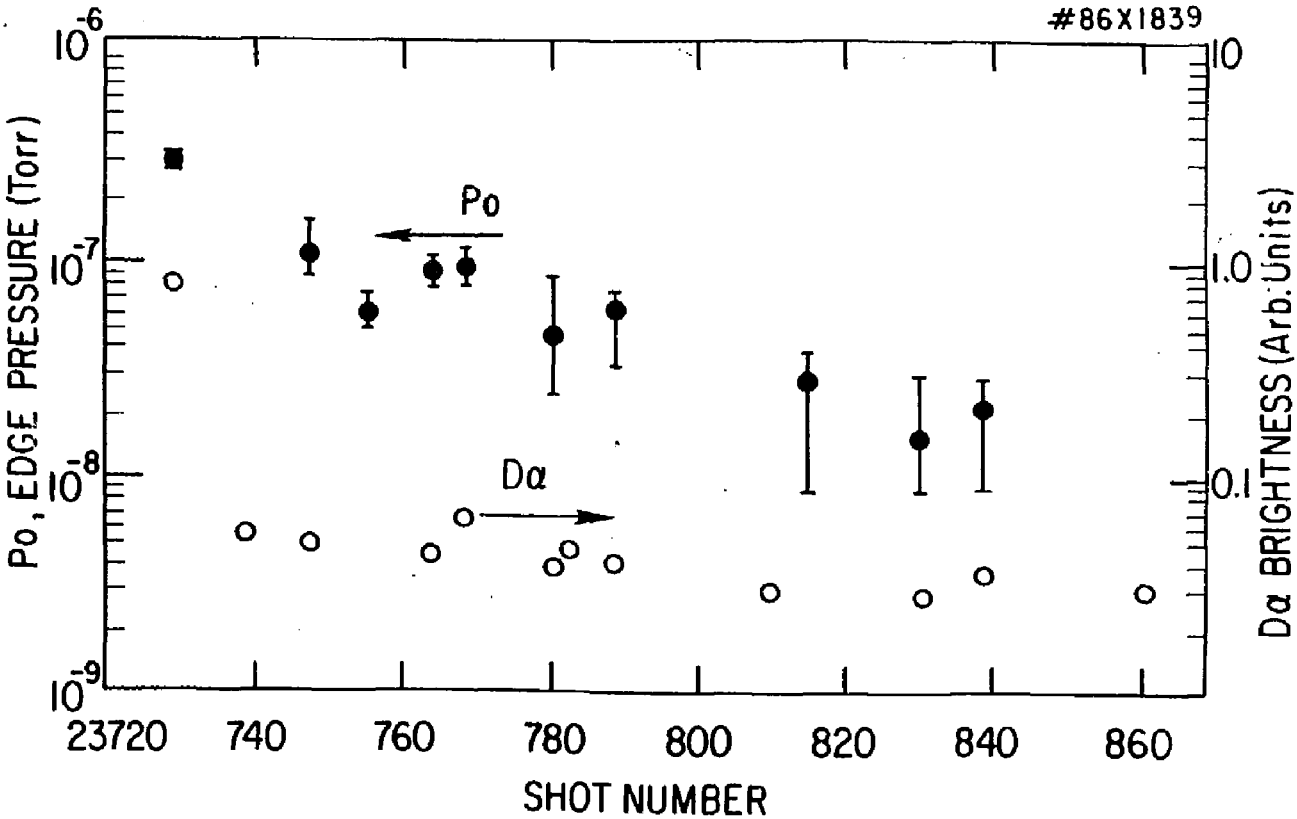
#86X1839
10^{-6}
10^{-7}
10^{-8}
10^{-9}
Po, EDGE PRESSURE (Torr)
Po
Dα
10
1.0
0.1
Dα BRIGHTNESS (Arb. Units)
23720
740
760
780
800
820
840
860
SHOT NUMBER

Fig. 8

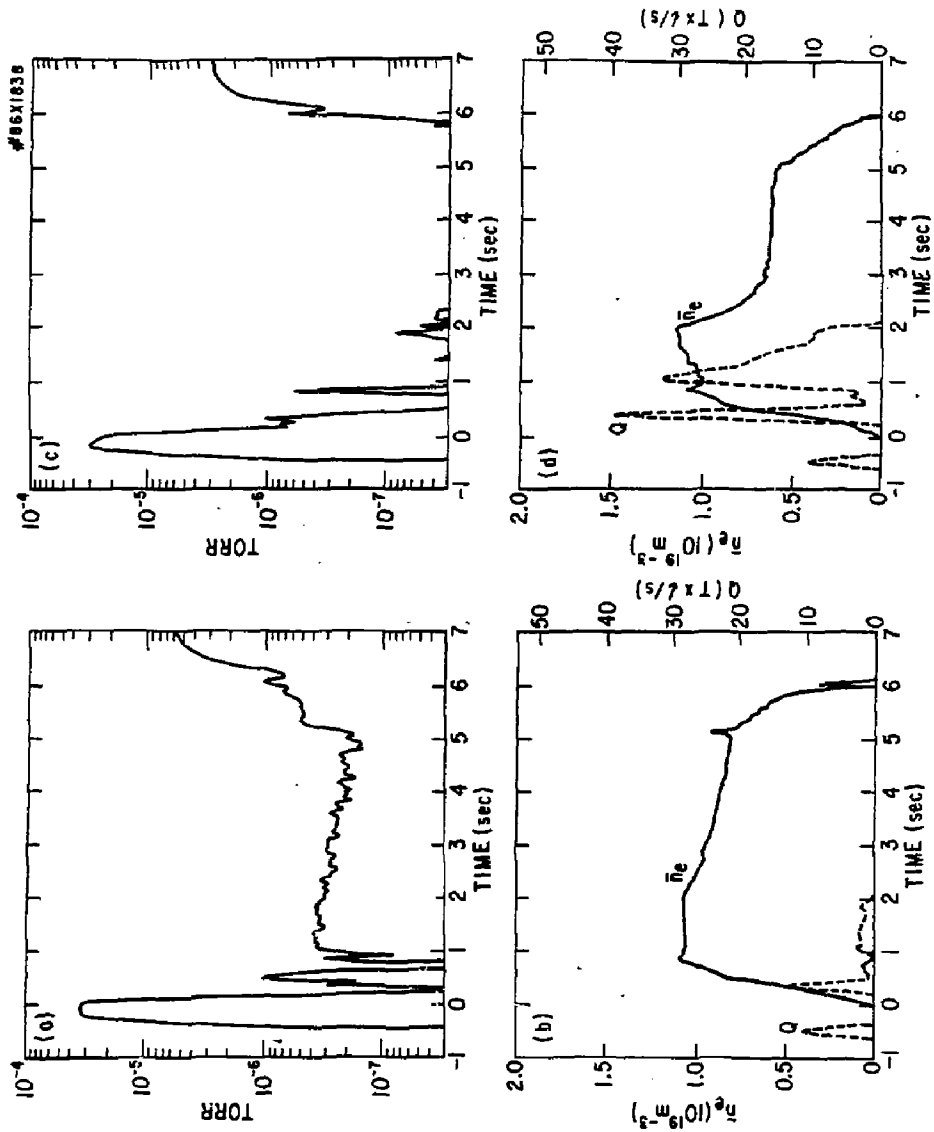

Fig. 9

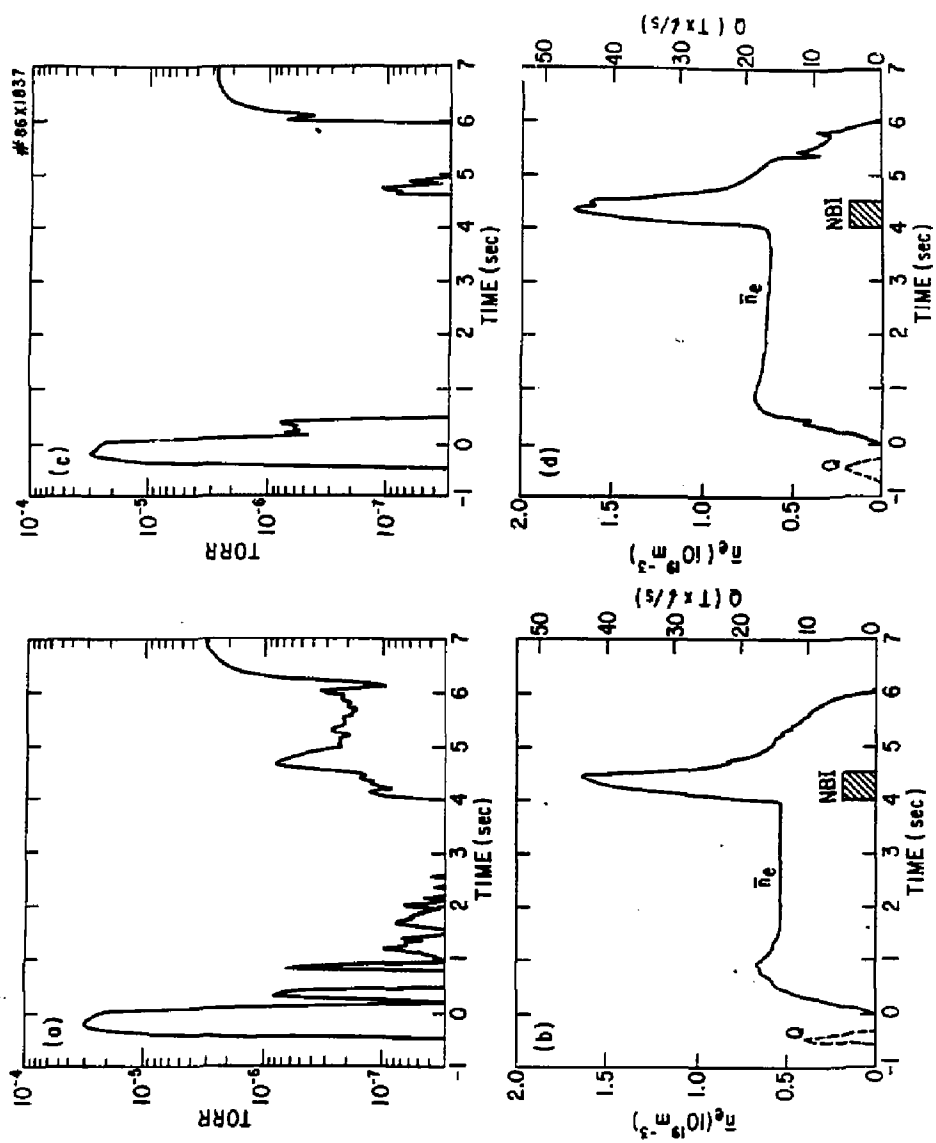

Fig. 10

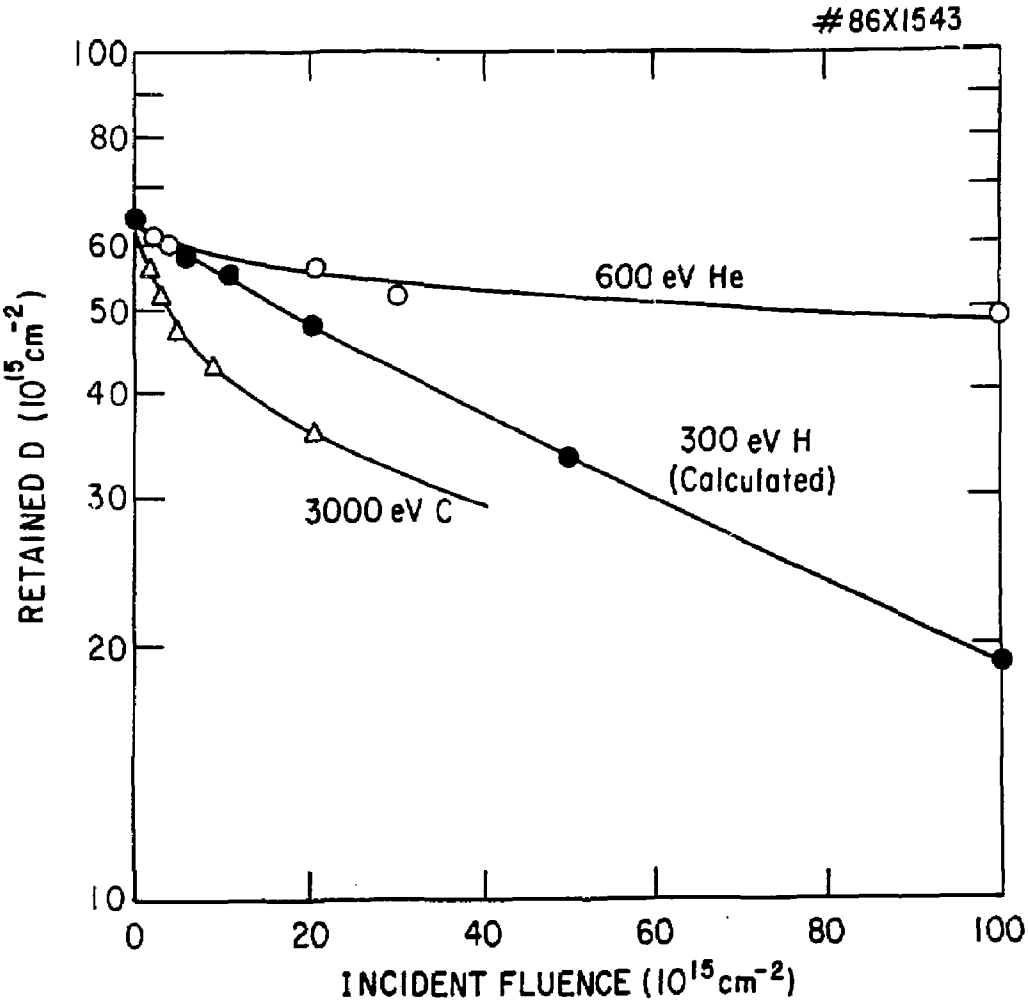
#86X1543
100
80
60
50
40
30
20
10
RETAINED D ($10^{15}cm^{-2}$)
600 eV He
300 eV H
(Calculated)
3000 eV C
0
20
40
60
80
100
INCIDENT FLUENCE ($10^{15}cm^{-2}$)

Fig. 11

EXTERNAL DISTRIBUTION IN ADDITION TO UC-20

Dr. Frank J. Paoloni, Univ of Wollongong, AUSTRALIA
Prof. M.H. Brennan, Univ Sydney, AUSTRALIA
Plasma Research Lab., Australian Nat. Univ., AUSTRALIA
Prof. I.R. Jones, Flinders Univ., AUSTRALIA
Prof. F. Cap, Inst Theo Phys, AUSTRIA
Prof. M. Heindler, Institut fur Theoretische Physik, AUSTRIA
M. Goossens, Astronomisch Instituut, BELGIUM
Ecole Royale Militaire, Lab de Phys Plasmas, BELGIUM
Com. of European, Dg XII Fusion Prog, BELGIUM
Prof. R. Boucique, Laboratorium voor Natuurkunde, BELGIUM
Dr. P.H. Sakanaka, Univ Estadual, BRAZIL
Instituto De Pesquisas Espaciasi-INPE, BRAZIL
Library, Atomic Energy of Canada Limited, CANADA
Dr. M.P. Bachynski, MPB Technologies, Inc., CANADA
Dr. H.M. Skarsgard, Univ of Saskatchewan, CANADA
Dr. H. Barnard, University of British Columbia, CANADA
Prof. J. Teichmann, Univ. of Montreal, CANADA
Prof. S.R. Sreenivasan, University of Calgary, CANADA
Prof. Tudor W. Johnston, INRS-Energie, CANADA
Dr. C.R. James, Univ. of Alberta, CANADA
Dr. Peter Lukac, Komenskeho Univ, CZECHOSLOVAKIA
The Librarian, Culham Laboratory, ENGLAND
Mrs. S.A. Hutchinson, JET Library, ENGLAND
C. Mouttet, Lab. de Physique des Milieux Ionises, FRANCE
J. Radet, CEN/CADARACHE - Bat 506, FRANCE
Dr. Tom Mual, Academy Bibliographic, HONG KONG
Preprint Library, Cent Res Inst Phys, HUNGARY
Dr. B. Desgupta, Saha Inst, INDIA
Dr. R.K. Chhajlani, Vikram Univ. INDIA
Dr. P. Kaw, Institute for Plasma Research, INDIA
Dr. Phillip Rosenau, Israel Inst Tech, ISRAEL
Prof. S. Cuperman, Tel Aviv University, ISRAEL
Librarian, Int'l Ctr Theo Phys, ITALY
Prof. G. Rostagni, Univ Di Padova, ITALY
Miss Clelia De Palo, Assoc EURATOM-ENEA, ITALY
Biblioteca, del CNR EURATOM, ITALY
Dr. H. Yamato, Toshiba Res & Dev, JAPAN
Prof. I. Kawakami, Atomic Energy Res. Institute, JAPAN
Prof. Kyoji Nishikawa, Univ of Hiroshima, JAPAN
Direc. Dept. Lg. Tokamak Res. JAERI, JAPAN
Prof. Satoshi Itoh, Kyushu University, JAPAN
Research Info Center, Nagoya University, JAPAN
Prof. S. Tanaka, Kyoto University, JAPAN
Library, Kyoto University, JAPAN
Prof. Nobuyuki Inoue, University of Tokyo, JAPAN
S. Mori, JAERI, JAPAN
M.H. Kim, Korea Advanced Energy Research Institute, KOREA
Prof. D.I. Choi, Adv. Inst Sci & Tech, KOREA
Prof. B.S. Liley, University of Waikato, NEW ZEALAND
Institute of Plasma Physics, PEOPLE'S REPUBLIC OF CHINA
Librarian, Institute of Phys., PEOPLE'S REPUBLIC OF CHINA
Library, Tsing Hua University, PEOPLE'S REPUBLIC OF CHINA
Z. Li, Southwest Inst. Physics, PEOPLE'S REPUBLIC OF CHINA
Prof. J.A.C. Cabral, Inst Superior Tecn, PORTUGAL
Dr. Octavian Petrus, AL I CUZA University, ROMANIA
Dr. Johan de Villiers, Plasma Physics, AEC, SO AFRICA
Prof. M.A. Hellberg, University of Natal, SO AFRICA
Fusion Div. Library, JEN, SPAIN
Dr. Lennart Stenflo, University of UMEA, SWEDEN
Library, Royal Inst Tech, SWEDEN
Prof. Hans Wilhelmson, Chalmers Univ Tech, SWEDEN
Centre Phys des Plasmas, Ecole Polytech Fed, SWITZERLAND
Bibliotheek, Fom-Inst Voor Plasma-Fysica, THE NETHERLANDS
Dr. D.D. Ryutov, Siberian Acad Sci, USSR
Dr. G.A. Eliseev, Kurchatov Institute, USSR
Dr. V.A. Glukhikh, Inst Electro-Physical, USSR
Dr. V.T. Tolok, Inst. Phys. Tech. USSR
Dr. L.M. Kovrizhnykh, Institute Gen. Physics, USSR
Prof. T.J.M. Boyd, Univ College N Wales, WALES
Nuclear Res. Establishment, Julich Ltd., W. GERMANY
Bibliothek, Inst. Fur Plasmaforschung, W. GERMANY
Dr. K. Schindler, Ruhr Universitat, W. GERMANY
ASDEX Reading Rm, IPP/Max-Planck-Institut fur Plasmaphysik, W. GERMANY
Librarian, Max-Planck Institut, W. GERMANY
Prof. R.K. Janev, Inst Phys, YUGOSLAVIA